Forward/Reverse Velocity and Acceleration Analysis for a Class of Lower-Mobility Parallel Mechanisms

Si J. Zhu
e-mail: zhusj@ysu.edu.cn

Zhen Huang[1]
e-mail: huangz@ysu.edu.cn

Hua F. Ding
e-mail: dhf@ysu.edu.cn

Robotics Research Center,
Mechanical Engineering College,
Yanshan University,
Qinhuangdao City, Hebei 066004, P.R. China

This paper proposes a novel kinematic analysis method for a class of lower-mobility mechanisms whose degree-of-freedom (DoF) equal the number of single-DoF kinematic pairs in each kinematic limb if all multi-DoF kinematic pairs are substituted by the single one. For such an **N**-*DoF* (**N**<6) *mechanism, this method can build a square* (**N**×**N**) *Jacobian matrix and cubic* (**N**×**N**×**N**) *Hessian matrix. The formulas in this method for different parallel mechanisms have unified forms and consequently the method is convenient for programming. The more complicated the mechanism is (for instance, the mechanism has more kinematic limbs or pairs), the more effective the method is. In the rear part of the paper, mechanisms 5-DoF 3-R*(*CRR*) *and 5-DoF 3-*(*RRR*)(*RR*) *are analyzed as examples.* [DOI: 10.1115/1.2429698]

Keywords: kinematic influence coefficient, lower-mobility, parallel mechanism, Jacobian, Hessian

1 Introduction

According to the number of degrees of freedom (DoF), parallel mechanisms (PMs) can be classified into three classes: lower-mobility PM (DoF<6), 6-DoF PM, and redundant PM (DoF >6). In recent years, the research point has been evolving from the 6-DoF PM to the lower-mobility PM for that the latter has simpler structure. In this period, many lower-mobility PMs are proposed [1–13].

Among these mechanisms, there is a class of mechanisms whose number of single-DoF kinematic pairs in every kinematic limb equals the DoF of the mechanism (**N**), such as **3-DoF**: planar 3-*RRR*, 3-*RPR*, spherical 3-*RRR*; **4-DoF**: ten mechanisms proposed by Li and Huang [7]; 14 by Kong and Gosselin [8]; 4-*RPPR* by Li [9]; **5-DoF**: 3-*RCRR*, 3-*RTRR* [10] by Huang and Li; 5-*RRRRR* by Fang and Tsai [11]; 30 mechanisms by Li et al. [12]; 16 by Kong and Gosselin [13], etc.

Conventional Jacobian for an **N**-DoF PM (**N**<6) is not a square matrix (6×**N**), which adds obstacles to kinematic modeling. Based on the kinematic influence coefficient (KIC) method for 6-DoF PMs [14,15], Yan and Huang proposed virtual mechanism principle (VMP) for lower-mobility PMs [16]. The VMP can build a square Jacobian (6×6) matrix and cubic Hessian (6×6 ×6) matrix by adding several virtual single-DoF kinematic pairs until every kinematic limb of PM has six single-DoF kinematic pairs. Rates of these virtual kinematic pairs have to be zero in order to guarantee that kinematic solutions of the virtual mechanism are equivalent to that of the initial one. Schilling [17] used the generalized inverse to work out joint rates in terms of the desired velocity in Cartesian space. Di Gregorio [5,18,19] analyzed the kinematics of several lower-mobility PMs through vector relationship. Considering the kinematic constraint, Joshi and Tsai [20] employed the reciprocal screw in Jacobian analysis where the Jacobians of constraints and actuations are used to build a square (6×6) overall Jacobian. Fang and Tsai [21] presented the reverse velocity analysis for lower-mobility serial mechanism with the reciprocal screw. Hernández [22] built a velocity equation based on a geometric matrix. Li et al. [23] derived a 5×5 Jacobian for some 5-DoF 3R2T PM in a special coordinate frame and one component of the velocity vector has to be zero. Hitoshi et al. [24] applied Lie algebra to the reverse kinematic analysis forserial manipulators. Lu [25] solved velocity and acceleration of parallel manipulators with 3–5 linear driving limbs with computer aided design (CAD) variation geometry.

In this paper, a novel method is proposed for forward/reverse kinematic analysis including not only the velocity but also acceleration analysis for the class of mechanisms mentioned above. Jacobian and Hessian matrices for an **N**-DoF PM (**N**<6) in this method are **N**×**N** and **N**×**N**×**N** matrices, respectively. Then the order of the Jacobian is less than 6 and its determinant of the Jacobian expressed by symbol variables is simpler than that of the Jacobian whose order is 6. This method can solve not only the case illustrated in Ref. [23], but also the case where all six components of the velocity vector as well as the acceleration vector are nonzero.

Moreover, the difficulty in achieving a velocity equation with the conventional method depends on the complexity of the geometrical relationship for a mechanism. The more complicated the mechanism is (for example, the mechanism has more limbs and kinematic pairs), the more complex the geometrical relationship is. So it is harder to achieve the velocity relationship with the conventional method if the mechanism is more complicated. Comparing with the traditional method, the method in this paper has the same difficulty for different mechanisms. So, the more complicated the mechanism is, the more effective the method is.

2 Kinematic Modeling

In the KIC method for a 6-DoF PM [14,15,26], Jacobian and Hessian matrices for a PM are built on the basis of Jacobian and Hessian matrices for limbs. In this study, Jacobian and Hessian matrices for a lower-mobility PM are also built in the same way.

[1]Corresponding author.

Contributed by the Mechanisms and Robotics Committee of ASME for publication in the Journal of Mechanical Design. Manuscript received June 8, 2005; final manuscript received April 11, 2006. Review conducted by Hashem Ashrafiuon.

2.1 Velocity Analysis

2.1.1 Forward Velocity Analysis for a Limb. For an **N**-DoF (**N**<6) PM, one kinematic limb can be considered as a serial mechanism. At first, substitute several single-DoF kinematic pairs for every multiple-DoF kinematic pair. For example, replace a cylindrical pair with a revolute and a coaxial prismatic pairs. Since every kinematic limb has **N** single-DoF kinematic pairs as mentioned above, the forward velocity equation for the ith kinematic limb is [14]

$$\boldsymbol{V}=\boldsymbol{J}^{(i)}\dot{\boldsymbol{\varphi}}^{(i)} \tag{1}$$

where

$$\boldsymbol{V}=[\omega_x \quad \omega_y \quad \omega_z \quad \nu_{px} \quad \nu_{py} \quad \nu_{pz}]^T \tag{2}$$

$$\boldsymbol{J}^{(i)}=[\$_1^{(i)} \quad \$_2^{(i)} \quad \cdots \quad \$_N^{(i)}] \tag{3}$$

$\boldsymbol{V}\in\boldsymbol{R}^{6\times1}$ denotes the velocity vector of the movable platform; $\boldsymbol{J}^{(i)}\in\boldsymbol{R}^{6\times N}$ the Jacobian for the ith kinematic limb; $\dot{\boldsymbol{\varphi}}^{(i)}\in\boldsymbol{R}^{N\times1}$ the velocity vector of the ith kinematic limb; ω_x the angular velocity component of the movable platform around the $\boldsymbol{x}$ axis; ν_{px} the linear velocity component of the point P on the movable platform along the $\boldsymbol{x}$ axis; and $\$_j^{(i)}\in\boldsymbol{R}^{6\times1}$ the unit screw of the jth kinematic pair in the ith kinematic limb.

Since the $\boldsymbol{J}^{(i)}$ is a $6\times\mathbf{N}$ matrix, the rank of $\boldsymbol{J}^{(i)}$ is **N** generally. Draw out any **N** independent rows from $\boldsymbol{J}^{(i)}$ and form a nonsingular square matrix named $\boldsymbol{J}_l^{(i)}$, where

$$\boldsymbol{J}_l^{(i)}=\begin{bmatrix}\boldsymbol{J}_{j_1:}^{(i)}\\ \boldsymbol{J}_{j_2:}^{(i)}\\ \vdots\\ \boldsymbol{J}_{j_N:}^{(i)}\end{bmatrix}\in\boldsymbol{R}^{N\times N} \tag{4}$$

$\boldsymbol{J}_{j_x:}^{(i)}$ denotes the (j_x)th row of the matrix $\boldsymbol{J}^{(i)}$ $(1\le j_x\le 6)$. Draw out **N** components from velocity vector $\boldsymbol{V}$ corresponding to the rows drawn out from $\boldsymbol{J}^{(i)}$ and build a new vector $\boldsymbol{V}_l$

$$\boldsymbol{V}_l=[V_1 \quad V_2 \quad \cdots \quad V_N]^T\in\boldsymbol{R}^{N\times l} \tag{5}$$

Then it is obvious that

$$\boldsymbol{V}_l=\boldsymbol{J}_l^{(i)}\dot{\boldsymbol{\varphi}}^{(i)} \tag{6}$$

2.1.2 Reverse Velocity Analysis for a Limb. The reverse form of Eq. (6) is

$$\dot{\boldsymbol{\varphi}}^{(i)}=[\boldsymbol{J}_l^{(i)}]^{-1}\boldsymbol{V}_l \tag{7}$$

2.1.3 Reverse Velocity Analysis for Mechanism. The generalized input velocity vector for the lower-mobility PM is

$$\dot{\boldsymbol{q}}=[\dot{q}_1 \quad \dot{q}_2 \quad \cdots \quad \dot{q}_N]^T=[\dot{\varphi}_{j_1}^{(i_1)} \quad \dot{\varphi}_{j_2}^{(i_2)} \quad \cdots \quad \dot{\varphi}_{j_N}^{(j_N)}]^T \tag{8}$$

where $\dot{\phi}_j^{(i)}$ is the velocity of the jth kinematic pair in the ith kinematic limb.

According to Eq. (7)

$$\dot{\varphi}_j^{(i)}=[\boldsymbol{J}_l^{(i)}]_{j:}^{-1}\boldsymbol{V}_l \tag{9}$$

where $[\boldsymbol{J}_l^{(i)}]_j^{-1}$ denotes the jth row of the inverse matrix of $\boldsymbol{J}_l^{(i)}$. Then the reverse velocity equation for the mechanism is

$$\dot{\boldsymbol{q}}=\boldsymbol{J}_{ls}^{-1}\boldsymbol{V}_l \tag{10}$$

where

$$\boldsymbol{J}_{ls}^{-1}=\begin{bmatrix}[\boldsymbol{J}_l^{(i_1)}]_{j_1:}^{-1}\\ [\boldsymbol{J}_l^{(i_2)}]_{j_2:}^{-1}\\ \vdots\\ [\boldsymbol{J}_l^{(i_N)}]_{j_N:}^{-1}\end{bmatrix}\in\boldsymbol{R}^{N\times N} \tag{11}$$

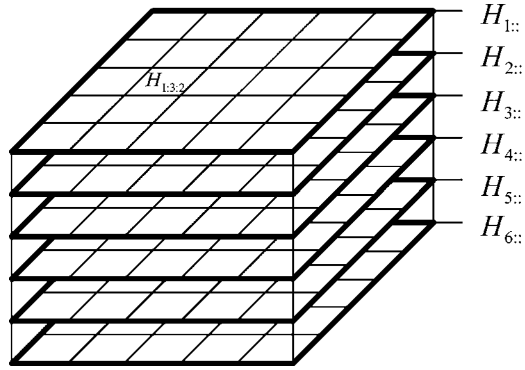

Fig. 1 Hessian for a 5-DoF mechanism

2.1.4 Forward Velocity Analysis for Mechanism. The reverse form of Eq. (10) is as follows

$$\boldsymbol{V}_l=\boldsymbol{J}_{ls}\dot{\boldsymbol{q}} \tag{12}$$

Generally, the rank of the matrix $\boldsymbol{J}^{(i)}$ is **N**, so the other 6-**N** rows of $\boldsymbol{J}^{(i)}$ can be linearly expressed by **N** rows which belong to $\boldsymbol{J}_l^{(i)}$. In other words, there exists

$$\boldsymbol{J}_{k:}^{(i)}=a\boldsymbol{J}_{j_1:}^{(i)}+b\boldsymbol{J}_{j2:}^{(i)}+\cdots+f\boldsymbol{J}_{j_N:}^{(i)} \tag{13}$$

where $\boldsymbol{J}_{k:}^{(i)}$ denotes the row of $\boldsymbol{J}$ which does not belong to $\boldsymbol{J}_l$; coefficients $a,b,\ldots,f$ are functions of position variables $\boldsymbol{\varphi}^{(i)}$ and exists

$$[a,b,\ldots,f]=\boldsymbol{J}_{k:}^{(i)}\begin{bmatrix}\boldsymbol{J}_{j_1:}^{(i)}\\ \boldsymbol{J}_{j_2:}^{(i)}\\ \vdots\\ \boldsymbol{J}_{j_N:}^{(i)}\end{bmatrix}^{-1} \tag{14}$$

Let $\boldsymbol{V}_k$ denote the component of $\boldsymbol{V}$ which does not belong to $\boldsymbol{V}_l$. In other words, $\boldsymbol{V}$ is the combination of $\boldsymbol{V}_l$ and 6-**N**$\boldsymbol{V}_k$s, and

$$\boldsymbol{V}_k=\boldsymbol{J}_{k:}^{(i)}\dot{\boldsymbol{\varphi}}=[a\boldsymbol{J}_{j_1:}^{(i)}+b\boldsymbol{J}_{j_2:}^{(i)}+\cdots+f\boldsymbol{J}_{j_N:}^{(i)}]\dot{\boldsymbol{\varphi}}=a\boldsymbol{V}_1+b\boldsymbol{V}_2+\cdots+f\boldsymbol{V}_N \tag{15}$$

So given $\boldsymbol{V}_l$, $\boldsymbol{V}_k$, and $\boldsymbol{V}$ are derivable.

Moreover, since $\boldsymbol{V}_l=\boldsymbol{J}_{ls}\dot{\boldsymbol{q}}=\boldsymbol{J}_l^{(i)}\dot{\boldsymbol{\varphi}}^{(i)}$

$$\dot{\boldsymbol{\varphi}}^{(i)}=[\boldsymbol{J}_l^{(i)}]^{-1}\boldsymbol{J}_{ls}\dot{\boldsymbol{q}} \tag{16}$$

Let $\boldsymbol{g}_l^{(i)}=[\boldsymbol{J}_l^{(i)}]^{-1}\boldsymbol{J}_{ls}\in\boldsymbol{R}^{N\times N}$, then

$$\dot{\boldsymbol{\varphi}}^{(i)}=\boldsymbol{g}_l^{(i)}\dot{\boldsymbol{q}} \tag{17}$$

2.2 Acceleration Analysis

2.2.1 Forward Acceleration Analysis for a Limb. The forward acceleration equation for the ith kinematic limb is [14]

$$\boldsymbol{A}=\boldsymbol{J}^{(i)}\ddot{\boldsymbol{\varphi}}^{(i)}+\dot{\boldsymbol{\varphi}}^{(i)^T}\boldsymbol{H}^{(i)}\dot{\boldsymbol{\varphi}}^{(i)} \tag{18}$$

where

$$\boldsymbol{A}=[\dot{\omega}_x \quad \dot{\omega}_y \quad \dot{\omega}_z \quad \dot{\nu}_{px} \quad \dot{\nu}_{py} \quad \dot{\nu}_{pz}]^T\in\boldsymbol{R}^{6\times1} \tag{19}$$

$\boldsymbol{A}$ denotes the acceleration vector of the movable platform; and $\boldsymbol{H}^{(i)}\in\boldsymbol{R}^{6\times N\times N}$ denotes the Hessian matrix for the ith kinematic limb. It is a three-dimensional vector which has six layers and each layer is an $\mathbf{N}\times\mathbf{N}$ matrix. Figure 1 illustrates the structure of Hessian matrix for a 5-DoF mechanism, which has six layers and each layer is a 5×5 matrix. $\ddot{\boldsymbol{\varphi}}^{(i)}\in\boldsymbol{R}^{N\times1}$ denotes the acceleration vector of the kinematic pairs in the ith kinematic limb; $\dot{\omega}_x$ denotes the angular acceleration component of movable platform around the $\boldsymbol{x}$ axis; and $\dot{\nu}_{px}$ denotes the linear acceleration component of the point P on the movable platform along the $\boldsymbol{x}$ axis. The jth component of $\boldsymbol{A}$ is

$$\boldsymbol{A}_j = \boldsymbol{J}_{j:}^{(i)}\ddot{\boldsymbol{\varphi}}^{(i)} + \dot{\boldsymbol{\varphi}}^{(i)^T}\boldsymbol{H}_{j::}^{(i)}\dot{\boldsymbol{\varphi}}^{(i)} \tag{20}$$

where $\boldsymbol{H}_{j::}^{(i)} \in \boldsymbol{R}^{N\times N}$ denotes the jth layer of the matrix $\boldsymbol{H}^{(i)}$.

Draw out those **N** layers of $\boldsymbol{H}^{(i)}$ corresponding to the rows drawn out in Eq. (4) and form a cubic matrix named $\boldsymbol{H}_l^{(i)}$

$$\boldsymbol{H}_l^{(i)} = \begin{bmatrix} \boldsymbol{H}_{j_1::}^{(i)} \\ \boldsymbol{H}_{j_2::}^{(i)} \\ \vdots \\ \boldsymbol{H}_{j_N::}^{(i)} \end{bmatrix} \in \boldsymbol{R}^{N\times N\times N} \tag{21}$$

Similar to Eq. (5), let

$$\boldsymbol{A}_l = [\boldsymbol{A}_1 \quad \boldsymbol{A}_2 \quad \cdots \quad \boldsymbol{A}_N]^T \in \boldsymbol{R}^{N\times 1} \tag{22}$$

then

$$\boldsymbol{A}_l = \boldsymbol{J}_l^{(i)}\ddot{\boldsymbol{\varphi}}^{(i)} + \dot{\boldsymbol{\varphi}}^{(i)^T}\boldsymbol{H}_l^{(i)}\dot{\boldsymbol{\varphi}}^{(i)} \tag{23}$$

2.2.2 Reverse Acceleration Analysis for a Limb. The reverse form of Eq. (23) is

$$\ddot{\boldsymbol{\varphi}}^{(i)} = [\boldsymbol{J}_l^{(i)}]^{-1}(\boldsymbol{A}_l - \dot{\boldsymbol{\varphi}}^{(i)^T}\boldsymbol{H}_l^{(i)}\dot{\boldsymbol{\varphi}}^{(i)}) \tag{24}$$

2.2.3 Reverse Acceleration Analysis for Mechanism. The generalized input acceleration vector for the lower-mobility PM is

$$\ddot{\boldsymbol{q}} = [\ddot{q}_1 \quad \ddot{q}_2 \quad \cdots \quad \ddot{q}_N]^T = [\ddot{\varphi}_{j_1}^{(i_1)} \quad \ddot{\varphi}_{j_2}^{(i_2)} \quad \cdots \quad \dot{\varphi}_{j_N}^{(i_N)}]^T \tag{25}$$

where $\ddot{\boldsymbol{\varphi}}_j^{(i)}$ is the input acceleration of the jth kinematic pair in the ith kinematic limb. According to Eq. (24),

$$\begin{aligned}\ddot{\boldsymbol{\varphi}}_j^{(i)} &= [\boldsymbol{J}_l^{(i)}]_{j:}^{-1}(\boldsymbol{A}_l - \dot{\boldsymbol{\varphi}}^{(i)^T}\boldsymbol{H}_l^{(i)}\dot{\boldsymbol{\varphi}}^{(i)}) \\ &= [\boldsymbol{J}_l^{(i)}]_{j:}^{-1}\boldsymbol{A}_l - \dot{\boldsymbol{\varphi}}^{(i)^T}([\boldsymbol{J}_l^{(i)}]_{j:}^{-1} * \boldsymbol{H}_l^{(i)})\dot{\boldsymbol{\varphi}}^{(i)}\end{aligned} \tag{26}$$

where the sign "*" denotes a generalized scalar product [15,27]. The generalized scalar product of two matrices $\boldsymbol{X} \in \boldsymbol{R}^{m\times n}$ and $\boldsymbol{Y} \in \boldsymbol{R}^{n\times p\times p}$ had been defined as follows

$$[\boldsymbol{X} * \boldsymbol{Y}]_{k::} = \sum_{l=1}^{n} \boldsymbol{X}_{kl}\boldsymbol{Y}_{l::} \in \boldsymbol{R}^{p\times p} \quad k = 1,2,\ldots,m \tag{27}$$

where $\boldsymbol{X}*\boldsymbol{Y} \in \boldsymbol{R}^{m\times p\times p}$; $\boldsymbol{X}_{kl}$ denotes the entry located at the kth row and lth column of the matrix $\boldsymbol{X}$.

Based on Eqs. (17), (25), and (26), the following equation can be derived

$$\ddot{\boldsymbol{q}} = [\boldsymbol{J}_{ls}]^{-1}\boldsymbol{A}_l - \begin{bmatrix} (\dot{\boldsymbol{q}}^T\boldsymbol{g}_l^{i_1^T})([\boldsymbol{J}_l^{(i_1)}]_{j_1:}^{-1} * \boldsymbol{H}_l^{(i_1)})(\boldsymbol{g}_l^{i_1}\dot{\boldsymbol{q}}) \\ (\dot{\boldsymbol{q}}^T\boldsymbol{g}_l^{i_2^T})([\boldsymbol{J}_l^{(i_2)}]_{j_2:}^{-1} * \boldsymbol{H}_l^{(i_2)})(\boldsymbol{g}_l^{i_2}\dot{\boldsymbol{q}}) \\ \vdots \\ (\dot{\boldsymbol{q}}^T\boldsymbol{g}_l^{(i_N)^T})([\boldsymbol{J}_l^{(i_N)}]_{j_N}^{-1} * \boldsymbol{H}_l^{(i_N)})(\boldsymbol{g}_l^{(i_N)}\dot{\boldsymbol{q}}) \end{bmatrix} \tag{28}$$

Then the reverse acceleration equation for the mechanism is

$$\ddot{\boldsymbol{q}} = \boldsymbol{J}_{ls}^{-1}\boldsymbol{A}_l - \dot{\boldsymbol{q}}^T\boldsymbol{H}_{ls}^{-1}\dot{\boldsymbol{q}} \tag{29}$$

where

$$\boldsymbol{H}_{ls}^{-1} = \begin{bmatrix} \boldsymbol{g}_l^{(i_1)^T}([\boldsymbol{J}_l^{(i_1)}]_{j_1}^{-1} * \boldsymbol{H}_l^{(i_1)})\boldsymbol{g}_l^{(i_1)} \\ \boldsymbol{g}_l^{(i_2)^T}([\boldsymbol{J}_l^{(i_2)}]_{j_2}^{-1} * \boldsymbol{H}_l^{(i_2)})\boldsymbol{g}_l^{(i_2)} \\ \vdots \\ \boldsymbol{g}_l^{(i_N)^T}([\boldsymbol{J}_l^{(i_N)}]_{j_N:}^{-1} * \boldsymbol{H}_l^{(i_N)})\boldsymbol{g}_l^{(i_N)} \end{bmatrix} \tag{30}$$

2.2.4 Forward Acceleration Analysis for Mechanism. The reverse form of Eq. (29) is

$$\boldsymbol{A}_l = \boldsymbol{J}_{ls}\ddot{\boldsymbol{q}} + \dot{\boldsymbol{q}}^T\boldsymbol{H}_{ls}\dot{\boldsymbol{q}} \tag{31}$$

where

$$\boldsymbol{H}_{ls} = \boldsymbol{J}_{ls} * \boldsymbol{H}_{ls}^{-1} \in \boldsymbol{R}^{N\times N\times N} \tag{32}$$

Furthermore, Hessian is the derivative of Jacobian about the position parameter $\boldsymbol{\varphi}^{(i)}$, namely

$$\boldsymbol{H}^{(i)} = \frac{\partial \boldsymbol{J}^{(i)}}{\partial \boldsymbol{\varphi}^{(i)}} \tag{33}$$

where $\boldsymbol{\varphi}^{(i)} = [\varphi_1^{(i)} \quad \varphi_2^{(i)} \quad \cdots \quad \varphi_N^{(i)}]^T$. Let $\boldsymbol{H}_{k::}^{(i)}$ denote the kth layer of $\boldsymbol{H}^{(i)}$ which does not belong to $\boldsymbol{H}_l$ shown in Eq. (21). Then

$$\begin{aligned}\boldsymbol{H}_{k::}^{(i)} &= \frac{\partial(\boldsymbol{J}_{k:}^{(i)})}{\partial \boldsymbol{\varphi}^{(i)}} \\ &= \frac{\partial(a\boldsymbol{J}_{j_1:}^{(i)} + b\boldsymbol{J}_{j_2:}^{(i)} + \cdots + f\boldsymbol{J}_{j_N:}^{(i)})}{\partial \boldsymbol{\varphi}} = a\frac{\partial(\boldsymbol{J}_{j_1:}^{(i)})}{\partial \boldsymbol{\varphi}^{(i)}} + b\frac{\partial(\boldsymbol{J}_{j_2:}^{(i)})}{\partial \boldsymbol{\varphi}^{(i)}} + \cdots \\ &\quad + f\frac{\partial(\boldsymbol{J}_{j_N:}^{(i)})}{\partial \boldsymbol{\varphi}^{(i)}} + \frac{\partial a}{\partial \boldsymbol{\varphi}^{(i)}}(\boldsymbol{J}_{j_1:}^{(i)}) + \frac{\partial b}{\partial \boldsymbol{\varphi}^{(i)}}(\boldsymbol{J}_{i_2:}^{(i)}) + \cdots + \frac{\partial f}{\partial \boldsymbol{\varphi}}(\boldsymbol{J}_{j_N:}^{(i)}) \\ &= [a \quad b \quad \cdots \quad f] * \boldsymbol{H}_l^{(i)} + \frac{\partial[a \quad b \quad \cdots \quad f]}{\partial \boldsymbol{\varphi}^{(i)}}\boldsymbol{J}_l^{(i)}\end{aligned} \tag{34}$$

According to Eqs. (13) and (34), $\boldsymbol{J}_{k:}^{(i)}$ and $\boldsymbol{H}_{k::}^{(i)}$ are derivable, then $\boldsymbol{A}_k$ and $\boldsymbol{A}$ are derivable, where $\boldsymbol{A}_k$ denotes the component of $\boldsymbol{A}$ does not belong to $\boldsymbol{A}_l$.

From the deduction above, it is obvious Eqs. (10), (12), (29), and (31) are the kinematic model of forward/reverse velocity and acceleration for the lower-mobility PM and they are built by Eqs. (6), (7), (23), and (24), respectively. Based on the uniform equations, the method is convenient for programming. For the forward analysis: DoF, mechanism parameters, and velocities/accelerations of actuators are the inputs of the program. The velocity/acceleration of the movable platform is the output of the program. For the reverse analysis: DoF, mechanism parameters, and velocity/acceleration of movable platform are the inputs of the program. The velocities/accelerations of actuators are the outputs of the program.

Note that the velocity and acceleration of any link in the PM can also be achieved. The detailed method will not be introduced here since it is similar to the kinematic influence coefficient method for a 6-DoF PM [15,26].

3 Mechanism Example

3.1 5-DoF 3-R(CRR)

3.1.1 Mechanism Description and Mobility Analysis. The base and movable platforms are connected by three kinematic limbs, each with three revolute joints and one cylindrical pair [12]. Both platforms are equilateral triangles. After kinematic equivalent substitution, each $R(CRR)$ limb can be represented with five single-DoF kinematic pairs as $R_1(P_2R_3R_4R_5)$. The pairs in parentheses intersect at one common point. The first joints ($\boldsymbol{R}_1$) of three kinematic limbs are perpendicular to the base platform. All other kinematic pairs' axes intersect at one point called rotation center. Rotations of three cylindrical pairs and the first revolute joints ($\boldsymbol{R}_1$) in the first and second kinematic limbs are chosen as input motions. The origin of the fixed coordinate frame $\boldsymbol{O}$-xyz is located at the center of the base platform; y axis passes through the points $\boldsymbol{P}_A$; z axis is perpendicular to the base platform and upward (see Fig. 2).

According to the screw theory [28], the screw system of the first kinematic limb under this structural condition is

$$\$_1 = [0,0,1;P_{Ay},0,0]$$

$$\$_2 = [0,0,0;0,1,0]$$

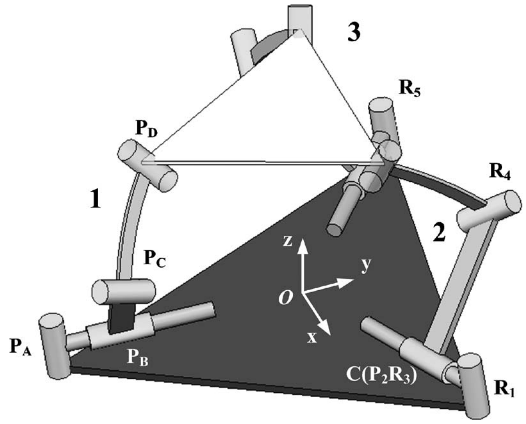

Fig. 2 Sketch of mechanism 3-*R*(*CRR*)

$$\$_3 = [0,1,0;0,0,0]$$

$$\$_4 = [l_4, m_4, n_4; 0,0,0]$$

$$\$_5 = [l_5, m_5, n_5; 0,0,0] \tag{35}$$

where $\$_i$ and (l_i, m_i, n_i) denote the unit-screw of the ith kinematic pair and its direction cosine, respectively; $\boldsymbol{P}_{Ay}$ denotes coordinate of point $\boldsymbol{P}_A$ on the y axis. Then the reciprocal screw [27] of the screw system expressed in Eq. (35) is

$$\$^r = [0,0,1;0,0,0] \tag{36}$$

If one screw denotes motion twist of a body, then its reciprocal screw denotes the constraint wrench acting on the body. From Eq. (36), $\$^r$ denotes constraint force (namely a constraint wrench with zero pitch) acting on the movable platform along the z axis. Similarly, the constraint forces from the other two kinematic limbs are the same with the first limb. Three constraint forces from three kinematic limbs are coaxial and form a “common constraint” which constrains the translation along the z axis.

Then, the mechanism rotation center can only translate in a plane parallel to the base plane and the movable platform can rotate only around the rotation center. In other words, the movable platform has three rotational freedoms and two translational freedoms in $\boldsymbol{o}$-$\boldsymbol{xy}$ plane, respectively. Under finite motion, the constraint wrench is the same as Eq. (36), so it is not an instantaneous mechanism. The number of DoF for the mechanism can also be verified by the modified *G-K* criterion [29]

$$\boldsymbol{M} = d(n-g-1) + \Sigma f + \nu - \zeta = 5(11-12-1) + 15 + 0 - 0 = 5 \tag{37}$$

Then, both numbers of DoF and single-DoF kinematic pairs in one limb are five (**N**=5).

3.1.2 Velocity Analysis. Since the five degrees of freedom include three rotational freedoms and two translational freedoms along $\boldsymbol{x}$ and $\boldsymbol{y}$ axes, let

$$\boldsymbol{V}_l = [\omega_x \quad \omega_y \quad \omega_z \quad \nu_{px} \quad \nu_{py}]^T \tag{38}$$

$$\boldsymbol{J}_l^{(i)} = \boldsymbol{J}_{(1-5):}^{(i)} \tag{39}$$

where $\boldsymbol{V}_l \in \boldsymbol{R}^{5\times 1}$; $\boldsymbol{J}_l^{(i)} \in \boldsymbol{R}^{5\times 5}$; $\boldsymbol{J}_{(1-5):}^{(i)}$ denotes the former five rows of matrix $\boldsymbol{J}^{(i)}$. Then its forward and reverse velocity analysis for the ith kinematic limb corresponding to Eqs. (6) and (7) are derivable.

Since rotations of three cylindrical pairs and the first revolute joints ($\mathbf{R}_1$) in the first and second kinematic limbs are chosen as the input motions. So the generalized input velocity vector for the lower-mobility 3-*R*(*CRR*) PM is

$$\dot{\boldsymbol{q}} = [\dot{\varphi}_1^{(1)} \quad \dot{\varphi}_3^{(1)} \quad \dot{\varphi}_1^{(2)} \quad \dot{\varphi}_3^{(2)} \quad \dot{\varphi}_3^{(3)}]^T \tag{40}$$

where

$$\dot{\varphi}_i^{(1)} = [\boldsymbol{J}_l^{(1)}]_{1:}^{-1}\boldsymbol{V}_l$$

$$\dot{\varphi}_3^{(1)} = [\boldsymbol{J}_l^{(1)}]_{3:}^{-1}\boldsymbol{V}_l$$

$$\dot{\varphi}_1^{(2)} = [\boldsymbol{J}_l^{(2)}]_{1:}^{-1}\boldsymbol{V}_l$$

$$\dot{\varphi}_3^{(2)} = [\boldsymbol{J}_l^{(2)}]_{3:}^{-1}\boldsymbol{V}_l$$

$$\dot{\varphi}_3^{(3)} = [\boldsymbol{J}_l^{(3)}]_{3:}^{-1}\boldsymbol{V}_l \tag{41}$$

So

$$\boldsymbol{J}_{ls}^{-1} = \begin{bmatrix} [\boldsymbol{J}_l^{(1)}]_{1:}^{-1} \\ [\boldsymbol{J}_l^{(1)}]_{3:}^{-1} \\ [\boldsymbol{J}_l^{(2)}]_{1:}^{-1} \\ [\boldsymbol{J}_l^{(2)}]_{3:}^{-1} \\ [\boldsymbol{J}_l^{(3)}]_{3:}^{-1} \end{bmatrix} \in \boldsymbol{R}^{5\times 5} \tag{42}$$

Then the forward and reverse velocity analysis for the mechanism corresponding to Eqs. (10) and (12) are derivable.

3.1.3 Acceleration Analysis. Similar with Eqs. (38) and (39), let

$$\boldsymbol{A}_l = \left[\dot{\omega}_x \quad \dot{\omega}_y \quad \dot{\omega}_z \quad \dot{\nu}_{px} \quad \dot{\nu}_{py}\right]^T \in \boldsymbol{R}^{5\times 1} \tag{43}$$

$$\boldsymbol{H}_l^{(i)} = \boldsymbol{H}_{(1-5)::}^{(i)} \in \boldsymbol{R}^{5\times 5\times 5} \tag{44}$$

where $\boldsymbol{H}_{(1-5)::}^{(i)}$ denotes five layers from the first one to the fifth one of $\boldsymbol{H}^{(i)}$. Then the forward and reverse acceleration analysis for the limb corresponding to Eqs. (23) and (24) are derivable.

Similar to Eq. (40), let the generalized input acceleration vector for the mechanism be

$$\ddot{\boldsymbol{q}} = \left[\ddot{\varphi}_1^{(1)} \quad \ddot{\varphi}_3^{(1)} \quad \ddot{\varphi}_1^{(2)} \quad \ddot{\varphi}_3^{(2)} \quad \ddot{\varphi}_3^{(3)}\right]^T \tag{45}$$

where

$$\ddot{\varphi}_{(1)}^{(1)} = [\boldsymbol{J}_l^{(1)}]_{1:}^{-1}(\boldsymbol{A}_l - \dot{\boldsymbol{\varphi}}^{(1)^T}\boldsymbol{H}_l^{(1)}\dot{\boldsymbol{\varphi}}^{(1)})$$

$$\ddot{\varphi}_{(3)}^{(1)} = [\boldsymbol{J}_l^{(1)}]_{3:}^{-1}(\boldsymbol{A}_l - \dot{\boldsymbol{\varphi}}^{(1)^T}\boldsymbol{H}_l^{(1)}\dot{\boldsymbol{\varphi}}^{(1)})$$

$$\ddot{\varphi}_{(1)}^{(2)} = [\boldsymbol{J}_l^{(2)}]_{3:}^{-1}(\boldsymbol{A}_l - \dot{\boldsymbol{\varphi}}^{(2)^T}\boldsymbol{H}_l^{(2)}\dot{\boldsymbol{\varphi}}^{(2)})$$

$$\ddot{\varphi}_{(3)}^{(2)} = [\boldsymbol{J}_l^{(2)}]_{3:}^{-1}(\boldsymbol{A}_l - \dot{\boldsymbol{\varphi}}^{(2)^T}\boldsymbol{H}_l^{(2)}\dot{\boldsymbol{\varphi}}^{(2)})$$

$$\ddot{\varphi}_{(3)}^{(3)} = [\boldsymbol{J}_l^{(3)}]_{3:}^{-1}(\boldsymbol{A}_l - \dot{\boldsymbol{\varphi}}^{(3)^T}\boldsymbol{H}_l^{(3)}\dot{\boldsymbol{\varphi}}^{(3)}) \tag{46}$$

So the reverse acceleration equation for the 3-*R*(*CRR*) PM is

$$\ddot{\boldsymbol{q}} = [\boldsymbol{J}_{ls}]^{-1}\boldsymbol{A}_l - \dot{\boldsymbol{q}}^T\boldsymbol{H}_{ls}^{-1}\dot{\boldsymbol{q}} \tag{47}$$

where

$$\boldsymbol{H}_{ls}^{-1} = \begin{bmatrix} \boldsymbol{g}_l^{(1)^T}([\boldsymbol{J}_l^{(1)}]_{1:}^{-1} * \boldsymbol{H}_l^{(1)})\boldsymbol{g}_l^{(1)} \\ \boldsymbol{g}_l^{(1)^T}([\boldsymbol{J}_l^{(1)}]_{3:}^{-1} * \boldsymbol{H}_l^{(1)})\boldsymbol{g}_l^{(1)} \\ \boldsymbol{g}_l^{(2)^T}([\boldsymbol{J}_l^{(2)}]_{1:}^{-1} * \boldsymbol{H}_l^{(2)})\boldsymbol{g}_l^{(2)} \\ \boldsymbol{g}_l^{(2)^T}([\boldsymbol{J}_l^{(2)}]_{3:}^{-1} * \boldsymbol{H}_l^{(2)})\boldsymbol{g}_l^{(2)} \\ \boldsymbol{g}_l^{(3)^T}([\boldsymbol{J}_l^{(3)}]_{3:}^{-1} * \boldsymbol{H}_l^{(3)})\boldsymbol{g}_l^{(3)} \end{bmatrix} \tag{48}$$

Then, the forward acceleration equation for the 3-*R*(*CRR*) PM is

$$\boldsymbol{A}_l = \boldsymbol{J}_{ls}\ddot{\boldsymbol{q}} + \dot{\boldsymbol{q}}^T\boldsymbol{H}_{ls}\dot{\boldsymbol{q}} \tag{49}$$

where

$$\boldsymbol{H}_{ls} = \boldsymbol{J}_{ls} * \boldsymbol{H}_{ls}^{-1} \in \boldsymbol{R}^{5\times 5\times 5} \tag{50}$$

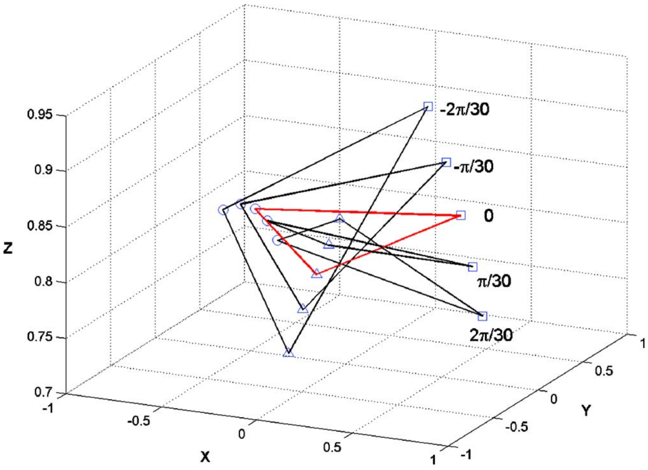

Fig. 3 Simulation of movable platform motion

3.1.4 Numerical Example. Let the side length of base platform r_{bp}=0.3 m; the side length of movable platform r_{mp}=0.1 m; both the angle between vector OP_B and OP_c and the angle between vector OP_C and OP_D be 47.2 deg; the maximum translational distance for three cylindrical pairs is 0.1 m. At the initial configuration when all five input angles are zero, the rotation center is coincident with the center of base platform. Now, let the input angle of first revolute pair in the first kinematic limb change in the range from −15 deg to 15 deg with an angular velocity of 1 rad/s. The other four actuators are locked. The input accelerations of five actuators are assumed to be zero, namely $\dot{\boldsymbol{q}}=[1\ \ 0\ \ 0\ \ 0\ \ 0]^T$ and $\ddot{\boldsymbol{q}}=[0\ \ 0\ \ 0\ \ 0\ \ 0]^T$.

According to Eqs. (13) and (34), all coefficients $a,b,\ldots,f$ are zero, so the component of linear velocity and acceleration vectors on the z axis are zero.

Figure 3 shows the locus of the movable platform, where angles in the figure indicate five different input angles. Figures 4 and 5 show the kinematic atlases including angular and linear velocity components and acceleration components, respectively. From Fig. 5, it is obvious that both components of linear velocity and acceleration vectors along the z axis vanish, which also confirms that the mechanism only has two independent translational freedoms.

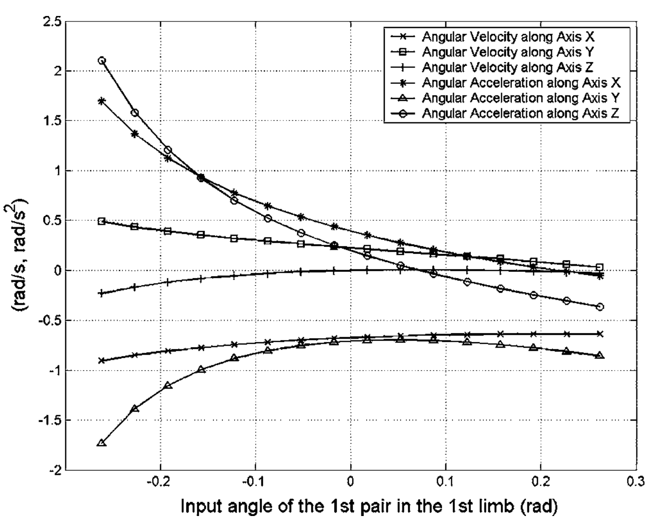

Fig. 4 Angular kinematics simulation

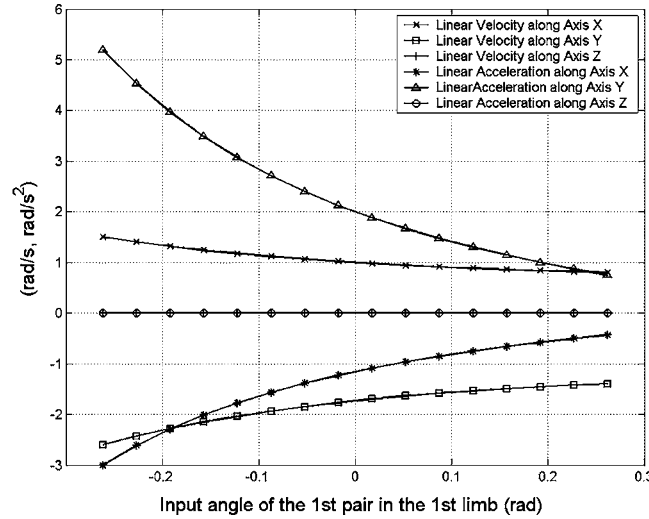

Fig. 5 Linear kinematics simulation: (a) parallel mechanism 3-(*RRR*)(*RR*); (b) one (*RRR*)(*RR*) limb at a general configuration

3.2 5-DoF 3-(*RRR*)(*RR*)

3.2.1 Mechanism Description and Mobility Analysis. The movable and base platforms are connected by three identical limbs each with five revolute joints [13]. Axes of three revolute joints adjacent to the base platform ($\mathbf{R}_1,\mathbf{R}_2,\mathbf{R}_3$) intersect at a point O_1 and the other two ($\mathbf{R}_4,\mathbf{R}_5$) intersect at another point O_2. The revolute pairs including $\mathbf{R}_1$ in three limbs and $\mathbf{R}_2$ in the first and second limbs are chosen as five input pairs (see Fig. 6).

Let point O_1 be the origin, the z axis perpendicular to the base platform, and the $\boldsymbol{x}$ axis pass through the center point of base pair $\mathbf{R}_1$. In such a reference coordinate frame, the screw system for the limb is

$$\$_1=[1,0,0;0,0,0]$$

$$\$_2=[l_2,m_2,n_2;0,0,0]$$

$$\$_3=[l_3,m_3,n_3;0,0,0]$$

$$\$_4=[l_4,m_4,n_4;\boldsymbol{O}_2\times\boldsymbol{S}_4]$$

$$\$_5=[l_5,m_5,n_5;\boldsymbol{O}_2\times\boldsymbol{S}_5] \tag{51}$$

where $\boldsymbol{O}_2=[x_{o2},y_{o2},z_{o2}]$ denotes the coordinates of the point $\boldsymbol{O}_2$.

The reciprocal screw of the screw system is a wrench with zero pitch

$$\$^r=[\boldsymbol{O}_2;0,0,0] \tag{52}$$

whose axis passes through both $\mathbf{O}_1$ and $\mathbf{O}_2$.

The reciprocal screws of three limbs are the same. So these constraints exerting on the movable platform form a common constraint, which is a wrench with zero pitch constraining the translational freedom along the line $\mathbf{O}_1\mathbf{O}_2$. So the movable platform has three rotational and two independent translational freedoms which can also be verified by modified *G-K* criterion [29]

$$\mathbf{M}=d(n-g-1)+\Sigma f+\nu-\zeta=5(14-15-1)+15+0-0=5 \tag{53}$$

Then, both numbers of DoF and single-DoF kinematic pairs in one limb are five ($\mathbf{N}$=5).

3.2.2 Velocity Analysis. In the fixed reference coordinate frame O_1-xyz, six components of velocity vector for the moving

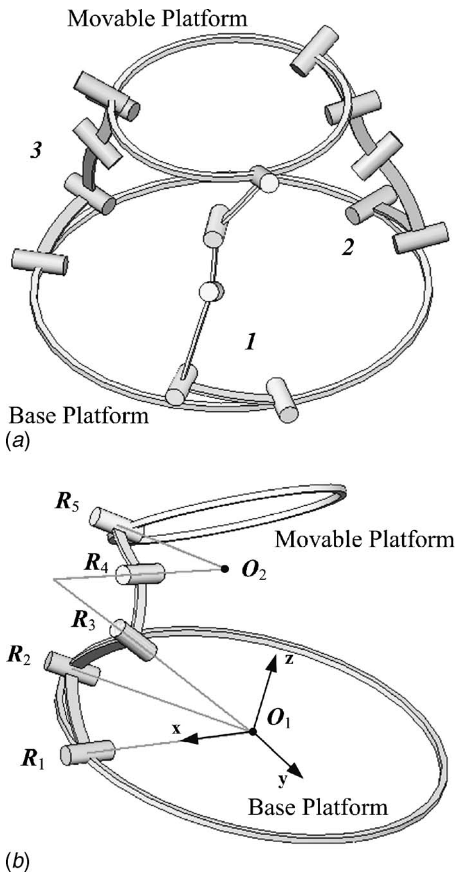

Fig. 6 Sketch of 3-(*RRR*)(*RR*)

platform are nonzero at general configuration as shown in the Fig. 6(*b*). There are six possibilities to draw five rows from six rows of $\boldsymbol{J}^{(i)}$ to build $\boldsymbol{J}_l$

$$(1)\ \boldsymbol{J}_l^{(i)} = [[\boldsymbol{J}_{1:}^{(i)}]^T, [\boldsymbol{J}_{2:}^{(i)}]^T, [\boldsymbol{J}_{3:}^{(i)}]^T, [\boldsymbol{J}_{4:}^{(i)}]^T, [\boldsymbol{J}_{5:}^{(i)}]^T]^T$$

$$(2)\ \boldsymbol{J}_l^{(i)} = [[\boldsymbol{J}_{1:}^{(i)}]^T, [\boldsymbol{J}_{2:}^{(i)}]^T, [\boldsymbol{J}_{3:}^{(i)}]^T, [\boldsymbol{J}_{4:}^{(i)}]^T, [\boldsymbol{J}_{6:}^{(i)}]^T]^T$$

$$(3)\ \boldsymbol{J}_l^{(i)} = [[\boldsymbol{J}_{1:}^{(i)}]^T, [\boldsymbol{J}_{2:}^{(i)}]^T, [\boldsymbol{J}_{3:}^{(i)}]^T, [\boldsymbol{J}_{5:}^{(i)}]^T, [\boldsymbol{J}_{6:}^{(i)}]^T]^T$$

$$(4)\ \boldsymbol{J}_l^{(i)} = [[\boldsymbol{J}_{1:}^{(i)}]^T, [\boldsymbol{J}_{2:}^{(i)}]^T, [\boldsymbol{J}_{4:}^{(i)}]^T, [\boldsymbol{J}_{5:}^{(i)}]^T, [\boldsymbol{J}_{6:}^{(i)}]^T]^T$$

$$(5)\ \boldsymbol{J}_l^{(i)} = [[\boldsymbol{J}_{1:}^{(i)}]^T, [\boldsymbol{J}_{3:}^{(i)}]^T, [\boldsymbol{J}_{4:}^{(i)}]^T, [\boldsymbol{J}_{5:}^{(i)}]^T, [\boldsymbol{J}_{6:}^{(i)}]^T]^T$$

$$(6)\ \boldsymbol{J}_l^{(i)} = [[\boldsymbol{J}_{2:}^{(i)}]^T, [\boldsymbol{J}_{3:}^{(i)}]^T, [\boldsymbol{J}_{4:}^{(i)}]^T, [\boldsymbol{J}_{5:}^{(i)}]^T, [\boldsymbol{J}_{6:}^{(i)}]^T]^T \tag{54}$$

Any $\boldsymbol{J}_l$ is valid as long as it is not singular. In this study, the $\boldsymbol{J}_{6:}$ will be the quasi-null row when $\mathbf{O}_1\mathbf{O}_2$ is nearly vertical to the base platform which will make the $\boldsymbol{J}_l$ quasi-singular. So the $\boldsymbol{J}_l$ without $\boldsymbol{J}_{6:}$ (the first one) is selected in this study. Then

$$\boldsymbol{V}_l = [\omega_x \quad \omega_y \quad \omega_z \quad \nu_{px} \quad \nu_{py}]^T \tag{55}$$

$$\boldsymbol{J}_l^{(i)} = \boldsymbol{J}_{(1-5):}^{(i)} \tag{56}$$

where $\boldsymbol{V}_l \in R^{5\times 1}$; $\boldsymbol{J}_l^{(i)} \in \boldsymbol{R}^{5\times 5}$. Then its forward and reverse velocity analysis for the *i*th kinematic limb corresponding to Eqs. (6) and (7) are derivable.

Input velocity vector for the 3-(*RRR*)(*RR*) PM is

$$\dot{\boldsymbol{q}} = [\dot{\varphi}_1^{(1)} \quad \dot{\varphi}_2^{(1)} \quad \dot{\varphi}_1^{(2)} \quad \dot{\varphi}_2^{(2)} \quad \dot{\varphi}_1^{(3)}]^T. \tag{57}$$

and reverse $\boldsymbol{J}_{ls}$ is

$$\boldsymbol{J}_{ls}^{-1} = \begin{bmatrix} [\boldsymbol{J}_l^{(1)}]_{1:}^{-1} \\ [\boldsymbol{J}_l^{(1)}]_{2:}^{-1} \\ [\boldsymbol{J}_l^{(2)}]_{1:}^{-1} \\ [\boldsymbol{J}_l^{(2)}]_{2:}^{-1} \\ [\boldsymbol{J}_l^{(3)}]_{1:}^{-1} \end{bmatrix} \in \boldsymbol{R}^{5\times 5} \tag{58}$$

Then, the forward and reverse velocity analysis for the mechanism corresponding to Eqs. (10) and (12) are derivable.

3.2.3 Acceleration Analysis. Similar to Eqs. (55) and (56), let

$$\boldsymbol{A}_l = [\dot{\omega}_x \quad \dot{\omega}_y \quad \dot{\omega}_z \quad \dot{\nu}_{px} \quad \dot{\nu}_{py}]^T \in \boldsymbol{R}^{5\times 1} \tag{59}$$

$$\boldsymbol{H}_l^{(i)} = \boldsymbol{H}_{(1-5)}^{(i)} \in \boldsymbol{R}^{5\times 5\times 5} \tag{60}$$

Then the forward and reverse acceleration analysis for the limb corresponding to Eqs. (23) and (24) is derivable.

Similar to Eq. (57), let the generalized input acceleration vector for the mechanism be

$$\ddot{\boldsymbol{q}} = [\ddot{\varphi}_1^{(1)} \quad \ddot{\varphi}_2^{(1)} \quad \ddot{\varphi}_1^{(2)} \quad \ddot{\varphi}_2^{(2)} \quad \ddot{\varphi}_1^{(3)}]^T \tag{61}$$

So the reverse acceleration equation for the 3-(*RRR*)(*RR*) PM is

$$\ddot{\boldsymbol{q}} = [\boldsymbol{J}_{ls}^{-1}]\boldsymbol{A}_l - \dot{\boldsymbol{q}}^T \boldsymbol{H}_{ls}^{-1} \dot{\boldsymbol{q}} \tag{62}$$

where

$$\boldsymbol{H}_{ls}^{-1} = \begin{bmatrix} \boldsymbol{g}_l^{(1)^T}([\boldsymbol{J}_l^{(1)}]_{1:}^{-1} * \boldsymbol{H}_l^{(1)})\boldsymbol{g}_l^{(1)} \\ \boldsymbol{g}_l^{(1)^T}([\boldsymbol{J}_l^{(1)}]_{2:}^{-1} * \boldsymbol{H}_l^{(1)})\boldsymbol{g}_l^{(1)} \\ \boldsymbol{g}_l^{(2)^T}([\boldsymbol{J}_l^{(2)}]_{1:}^{-1} * \boldsymbol{H}_l^{(2)})\boldsymbol{g}_l^{(2)} \\ \boldsymbol{g}_l^{(2)^T}([\boldsymbol{J}_l^{(2)}]_{2:}^{-1} * \boldsymbol{H}_l^{(2)})\boldsymbol{g}_l^{(2)} \\ \boldsymbol{g}_l^{(3)^T}([\boldsymbol{J}_l^{(3)}]_{1:}^{-1} * \boldsymbol{H}_l^{(3)})\boldsymbol{g}_l^{(3)} \end{bmatrix} \tag{63}$$

Then the forward acceleration equation for the 3-(*RRR*)(*RR*) PM is

$$\boldsymbol{A}_l = \boldsymbol{J}_{ls}\ddot{\boldsymbol{q}} + \dot{\boldsymbol{q}}^T \boldsymbol{H}_{ls} \dot{\boldsymbol{q}} \tag{64}$$

where

$$\boldsymbol{H}_{ls} = \boldsymbol{J}_{ls} * \boldsymbol{H}_{ls}^{-1} \in \boldsymbol{R}^{5\times 5\times 5} \tag{65}$$

3.2.4 Numerical Example. Limited by the length of the paper, this paper only give three numerical $\boldsymbol{J}^{(i)}$ $(i=1,2,3)$ and $\boldsymbol{J}_{ls}$, but no

Table 1 Numerical Jacobian matrices for limbs and J_{ls}

$\boldsymbol{J}^{(1)}$	=	1.0000	0.8660	0.5010	0.9990	0.8853
		0	0.0436	0.0319	0.0456	−0.3905
		0	0.4981	0.8649	−0.0022	0.2524
		0	0.9955	0.5921	0.0000	0.0000
		−25.9793	−22.4767	−12.9762	−0.0000	0.0000
		0.2743	0.2356	0.1360	0.0000	−0.0000
$\boldsymbol{J}^{(2)}$	=	−0.5000	−0.3578	−0.1967	−0.3963	−0.0478
		0.8660	0.7934	0.4682	0.9181	0.9189
		0	0.4924	0.8615	−0.0090	−0.3917
		22.4987	20.4772	11.9265	−0.0000	0.0000
		12.9896	9.3177	5.1482	−0.0000	0.0000
		−0.1754	−0.1332	−0.0746	0.0000	−0.0000
$\boldsymbol{J}^{(3)}$	=	−0.5000	−0.4330	−0.2432	−0.4809	−0.8375
		−0.8660	−0.7500	−0.4370	−0.8768	−0.5283
		0	0.5000	0.8660	−0.0000	0.1393
		−22.4987	−19.6216	−11.5893	0.0000	0.0000
		12.9896	11.2714	6.3572	−0.0000	−0.0000
		−0.0989	−0.0856	−0.0474	−0.0000	0.0000
$\boldsymbol{J}_{ls}$	=	0.9850	0.7847	−0.6715	−0.7965	0.0608
		−5.1017	−1.1574	7.6311	0.8468	0.6376
		1.3005	−0.3034	−4.7372	−0.5511	−0.3749
		−1.1626	−0.0296	−0.1467	−0.0214	−0.0000
		−0.5019	−0.0128	3.2145	0.4692	−0.0000

Hessian matrices, shown in Table 1. Let α_{mn} denote the angle between $\mathbf{R}_m$ and $\mathbf{R}_n$, $\alpha_{12}=\alpha_{23}=\alpha_{45}=\pi/6$, $\alpha_{34}=\pi/3$. Radii for base and movable platforms are 200 mm and 50 mm, respectively. Three numerical $\boldsymbol{J}(i)$ and $\boldsymbol{J}_l$ are given when $\varphi_1^{(1)}=17\pi/36$, $\varphi_2^{(1)}=\pi/36$, $\varphi_1^{(2)}=5\pi/9$, $\varphi_2^{(2)}=-\pi/18$, and $\varphi_1^{(3)}=\pi/2$.

4 Conclusions

This paper presents a novel method for the forward/reverse velocity and acceleration analysis of a class of lower-mobility parallel mechanisms whose number of single-DoF pairs in every limb equals the number of DoF for the mechanism. The method is based on the kinematic influence coefficient method for the 6-DoF parallel mechanism. With this method, orders of both Jacobian and Hessian for the lower-mobility PMs are less than 6, which make it easier to calculate the determinant of the symbol variable Jacobian. Another merit of this method is that forms of formulas are unified, so the method is convenient for programming. The more complicated the mechanism is, the more effective the method is.

Acknowledgment

The authors of this paper wish to acknowledge the support received from the NSFC with Grant No. 50275129. The authors also thank Dr. Joseph and Mr. Zhan Y. Ma for discussion on the paper and the anonymous reviewers for their useful comments.

References

[1] Hunt, K. H., 1983, "Structural Kinematics of In-parallel-actuated Robot-arms," ASME J. Mech., Transm., Autom. Des., **105**(4), pp. 705–712.

[2] Song, S. M., and Zhang, M. D., 1995, "A Study of Reactional Force Compensation Based on Three-degree-of-freedom Parallel Platforms," J. Rob. Syst., **12**(12), pp. 783–794.

[3] Merlet, J-P., 2000, *Parallel Robots*, Kluwer Academic, Dordrecht.

[4] Zlatanov, D., and Gosselin, C. M., 2001, "A New Parallel Architecture with Four Degrees of Freedom," Proceeding of the 2nd Workshop on Computational Kinematics, Seoul, Korea, May 20–22, pp. 57–66.

[5] Di Gregorio, R., 2002, "The 3-RRS Wrist: A New, Very Simple and Not Over Constrained Spherical Parallel Mechanism," Proceeding of 2002 ASME Design Engineering Technical Conferences, Montreal, Canada, Sept. 29–Oct. 2, MECH-34344.

[6] Kong, X. W., and Gosselin, C. M., 2002, "Kinematics and Singularity Analysis of a Novel Type of 3-CRR 3-DoF Translational Parallel Mechanism," Int. J. Robot. Res., **21**(9), pp. 791–798.

[7] Huang, Z., and Li, Q. C., 2003, "Type Synthesis of Symmetrical Lower-mobility Parallel Mechanisms Using the Constraint Synthesis Method," Int. J. Robot. Res., **22**(1), pp. 59–79.

[8] Kong, X. W., and Gosselin, C. M., 2004, "Type Synthesis of 3T1R 4-DOF Parallel Manipulators Based on Screw Theory," IEEE Trans. Rob. Autom., **20**(2), pp. 181–190.

[9] Li, S. H., 2004, "Some Theoretical Issues on Analysis and Synthesis of Lower-Mobility Parallel Mechanisms," Ph.D. dissertation, Engineering, Yanshan University, Qinhuangdao, Hebei, China (in Chinese).

[10] Huang, Z., and Li, Q. C., 2002, "General Methodology for Type Synthesis of Lower-Mobility Symmetrical Parallel Manipulators and Several Novel Manipulators," Int. J. Robot. Res., **21**(2), pp. 131–145.

[11] Fang, Y. F., and Tsai, L. W., 2002, "Structure Synthesis of a Class of 4-DoF and 5-DoF Parallel Manipulators with Identical Limb Structures," Int. J. Robot. Res., **21**(9), pp. 799–810.

[12] Li, Q. C., Huang, Z., and Hervé, J. M., 2004, "Type Synthesis of 3R2T 5-DOF Parallel Mechanisms Using the Lie Group of Displacements," IEEE Trans. Rob. Autom., **20**(2), pp. 173–180.

[13] Kong, X. W., and Gosselin, C. M., 2005, "Type Synthesis of 5-DOF Parallel Manipulators Based on Screw Theory," J. Rob. Syst., **22**(10), pp. 535–547.

[14] Thomas, M., and Tesar, D., 1982, "Dynamic Modeling of Serial Mechanism Arms," J. Dyn. Syst., Meas., Control, **104**(9), pp. 218–227.

[15] Huang, Z., 1985, "Modeling Formulation of 6-dof Multi-loop Parallel Mechanisms," Proceeding of the 4th IFToMM International Symposium on Linkage and Computer Aided Design Methods, Bucharest, Romania, Vol. II-1, pp. 155–162.

[16] Yan, J., and Huang, Z., 1985, "Kinematical Analysis of Multi-loop Spatial Mechanism," Proceeding of the 4th IFToMM International Symposium on Linkage and Computer Aided Design Methods, Bucharest, Romania, Sept. 16, Vol. II-2 pp. 439–446.

[17] Schilling, R. J., 1990, *Fundamentals of Robotics: Analysis and Control*, Prentice–Hall, Englewood Cliffs, NJ.

[18] Di Gregorio, R., 2000, "Closed-form Solution of the Position Analysis of the Pure Translational 3-RUU Parallel Mechanism," Proceeding of the 8th Symposium on Mechanisms and Mechanical Transmissions, MTM 2000, Timisoara, Romania, Oct. 19–22, pp. 119–124.

[19] Di Gregorio, R., 2003, "Kinematics of the 3-UPU Wrist," Mech. Mach. Theory, **38**(3), pp. 253–263.

[20] Joshi, S. A., and Tsai, L. W., 2002, "Jacobian Analysis of Mobility-deficient Parallel Mechanisms," Proceedings ASME 2002 Design Engineering Technical Conferences and Computer and Information in Engineering Conference, Montreal, Canada, Sept. 29–Oct. 2, MECH-34238.

[21] Fang, Y. F., and Tsai, L. W., 2003, "Inverse Velocity and Singularity Analysis of Low-DoF Serial Mechanisms," J. Rob. Syst., **20**(4), pp. 177–188.

[22] Hernández, A., Altuzarra, O., Avilés, R., et al., 2003, "Kinematic Analysis of Mechanisms via a Velocity Equation Based in a Geometric Matrix," Mech. Mach. Theory, **38**(12), pp. 1413–1429.

[23] Li, Q. C., Hu, X. D., and Huang, Z., 2004, "Jacobian Derivation of 5-DoF 3R2T Parallel Mechanisms," Proceedings ASME 2004 Design Engineering Technical Conferences and Computers and Information in Engineering Conference, Salt Lake City, UT, Sept. 28–Oct. 2, MECH-57276.

[24] Hitoshi, T., Takaaki, O., Norio, M., et al., 2004, "A Method to Solve Inverse Kinematics Problems Using Lie Algebra and Its Application to Robot Spray Painting Simulation," Proceedings ASME 2004 Design Engineering Technical Conferences and Computer and Information in Engineering Conference, Salt Lake City, UT, DAC-57086.

[25] Lu, Y., 2006, "Using CAD Variation Geometry for Solving Velocity and Acceleration of Parallel Manipulators with 3-5 Linear Driving Limbs," J. Mech. Des., **128**(4), pp. 738–746.

[26] Huang, Z., 1985, "Modeling Formulation of 6-dof Multi-loop Parallel Mechanisms," Proceeding of the 4th IFToMM International Symposium on Linkage and Computer Aided Design Methods, Bucharest, Romania, Sept. 16, Vol. II-1, pp. 163–170.

[27] Zhu, S. J., and Huang, Z., 2005, "Forward/Reverse Velocity and Acceleration Analyses for a Class of Lower-Mobility Parallel Mechanisms," Proceedings ASME 2005 Design Engineering Technical Conferences and Computer and Information in Engineering Conference, Long Beach, CA, Sept. 24–28, MECH-84081.

[28] Hunt, K. H., 1978, *Kinematic Geometry of Mechanisms*, Claredon, Oxford, U.K.

[29] Huang, Z., 2004, "Kinematics and Type Synthesis of Lower-mobility Parallel Robot Manipulators," Proceedings 11th IFToMM2004, Tianjin, China, Apr. 1–4, Technical Rep. 6, pp. 65–76.